The clamp bender
a new testing equipment for thin glass

Zaccaria, Marco; Peters, Timon; Ebert, Jan; Lucca, Nerio; Schneider, Jens; Louter, Christian

DOI
10.1007/s40940-022-00188-8

Publication date
2022

Document Version
Final published version

Published in
Glass Structures and Engineering

Glass Struct. Eng. (2022) 7:173–186
https://doi.org/10.1007/s40940-022-00188-8

RESEARCH PAPER

The clamp bender: a new testing equipment for thin glass

Marco Zaccaria · Timon Peters · Jan Ebert · Nerio Lucca · Jens Schneider · Christian Louter

Received: 13 May 2022 / Accepted: 13 June 2022 / Published online: 29 July 2022

Abstract The bending strength of flat glass panels including the effects of their edges, is commonly determined by means of the four-point bending test method. This is an established and reliable method. However, when testing glass thinner than 3 mm, large deformation may occur. This means that the calculated stresses might not correspond to the actual, as the hypothesis behind the small deformation theory does no longer hold. Furthermore, it might occur that the specimen slips out of the supports, compelling the testing impossible. An alternative method, suitable for thin glass, consists of inducing an increasing curvature from flat until fracture. The curvature is to be constant along the length of the specimen at any time. The stress at fracture is calculated by knowing the corresponding radius or the applied bending moment. The equipment capable of performing this test is the clamp bender whereby the glass is held by two clamps at the specimen's ends. Rotational and translational movement combine to uniaxially bend the glass as desired. This paper explores the validity of the clamp bender for testing thin glass by comparing the results generated by three different test setups developed at TU Darmstadt, TU Dresden and AGC. The three individually developed clamp bender setups follow the same principle, but present a few differences in actuation. Using these three clamp bender test setups, identical series of thin glass specimens were tested. The results showed that the glass fracture strength data coming from different setups match quite well one another. This paper discusses the different test setups and compares the obtained glass strength data. It contributes to the development of a universally applicable, simple and reliable test method for thin glass.

Keywords Thin glass · Clamp bender · Mechanical testing · Edge strength

M. Zaccaria (✉) · N. Lucca
AGC Glass Europe, Ottignies-Louvain-la-Neuve, Belgium
e-mail: marco.zaccaria@agc.com

T. Peters · J. Schneider
TU Darmstadt, Darmstadt, Germany

J. Ebert · C. Louter
TU Dresden, Dresden, Germany

C. Louter
TU Delft, Delft, The Netherlands

1 Introduction

Each year the vast majority of flat glass produced worldwide by the float process is in the thickness range 2–25 mm. Its use is mainly shared in the building and automotive sectors. Around the year 2007, smartphones were introduced in the market. The glass used for such devices is thinner than 2 mm and is commonly chemically strengthened to achieve outstanding mechanical properties. The combination of small thickness and mechanical properties allow for an unprecedented glass flexibility, which is an highly appealing feature for applications in architecture. Furthermore, there is an embedded sustainability feature in thin glass:

it could cover the same amount of surface as regular glass covers today (e.g. in facades), but with less material, without compromising on the performances. Designers and researchers started therefore to investigate the possibility of using thin glass in architecture. For example, Lambert and O'Callaghan (2013) deemed thin glass of great potential in the areas of cold-formed surfaces, tensile membrane structures and impact resistant transparent products. Pennetier et al. (2019) elaborated on concepts and design considerations while working on a thin glass sculpture. Few studies aimed at exploiting thin glass flexibility for movable structures. More specifically, Neugebauer et al. (2018) and Silveira et al. (2018) evaluated the possibility of having movable thin glass elements to control closing and opening of double skin façades. On the other hand, applications might also call for limited deformations. In this field, Louter et al. (2018) and Pfarr et al. (2021) investigate the possibilities of rigidifying thin glass panels by means of a 3D printed polymer core. Alternatively, glass could be rigidified by geometry: a thin-walled structure is capable to address mainly compressive load paths, suitable for glass, whilst limiting the deformation. This led Schlosser (2018) to evaluate cold bent application in monolithic and laminated form. When laminating thin glass with thicker glass or with plastics impressive mechanical performances can be achieved whilst also observing fail-safe behaviour or adding special features such as special connections. In particular, Overend et al. (2013) showed how strong a laminate assembly combining thin chemically strengthened glass with regular glass is. Cervio (2016), Weimar et al. (2018) and Hänig et al. (2021) investigated composite panels made of solid polymer cores (e.g. polycarbonate sheets, or cast-in-place polymethylmethacrylate) bonded with thin glass cover layers, investigating the impact resistance and how these panels can conveniently be connected by means of screws perforating the solid polymer core.

But what is exactly thin glass and why is it this strong? Glass between 0.5 and 2.1 mm of thickness is here considered thin glass. It can be produced by the down drawn process or more efficiently by the float process. The choice of production process depends mainly on the fusion temperature, which is function of the raw materials: an aluminosilicate glass composition requires 1600 °C which is prohibitive for a float line. However, a composition between aluminosilicate and soda-lime silica glass composition can be compatible with a float line, which is the case for Falcon glass, by AGC. The float production could be a key advantage to endorse thin glass in architecture due to its lower production cost and the larger stock size compared to the down drawn process. However, whether down drawn or float, as-produced thin glass is still glass with its intrinsic brittleness. It is only when subjecting it to the chemical strengthening process that it acquires extra strength. Chemical strengthening, also known as ion-exchange, consists of immersing the glass for a given soak time into a molten salt of potassium nitrate kept at a given temperature, the soak temperature (Bartholomew et al. 1980). Soak time commonly varies between 2 and 24 h, whilst soak temperature is normally kept at 460 °C (Zaccaria et al. 2019). During the process, the larger potassium ions in the molten salt replace the smaller sodium ions in the glass structure, inducing so a state of pre-compression across the glass thickness (residual stress profile, Fig. 1). The residual stress profile is characterized by a surface compression which decreases steeply and linearly towards the core where it turns into tension. The point where the compression changes to tension is known as depth of layer (DoL) or case depth. The surface compression and the case depth are the main parameters that drive the strength of chemically strengthened glass: the target is that the DoL would be larger than any pre-existing or usage-induced flaw (Zaccaria et al. 2021). In contrast, any flaw deeper than the DoL will severely affect its strength as its tip will be under the core tension (Datsiou et al. 2017). The kinetics of the ion-exchange are dependent on the ratio between the alkali-oxide and the aluminium oxide, γ, with the rate being faster when $\gamma \leq 1$ (Burggraaf et al. 1964). That explains why the chemical strengthening is more effective for aluminosilicate glasses than for soda-lime silica glasses. For reference, the potential of residual stress build-up and case depth for soda-lime silica, aluminosilicate and Falcon glass is shown in (Fig. 2). The surface residual stress and DoL can be measured non-destructively by means of photoelasticity, but the resulting glass strength has to be assessed by destructive methods (Zaccaria et al. 2016).

The bending strength of flat glass panels, including the effects of their edges, is commonly determined by means of the established four-point bending (4 PB) test method, regulated in Europe and US, by the respective standards (EN 1288-3 2016), (ASTM E1300 2012). The equipment to use for the 4 PB test must ensure:

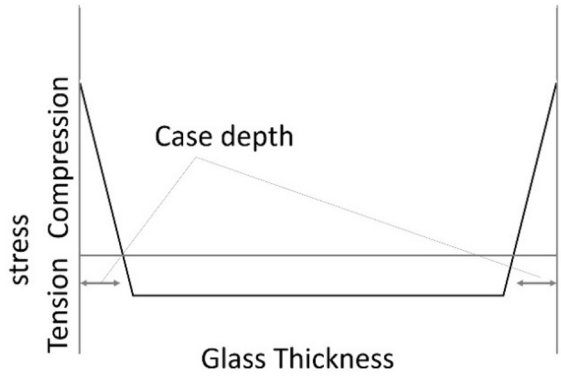

Fig. 1 Residual stress profile of chemically strengthened glass

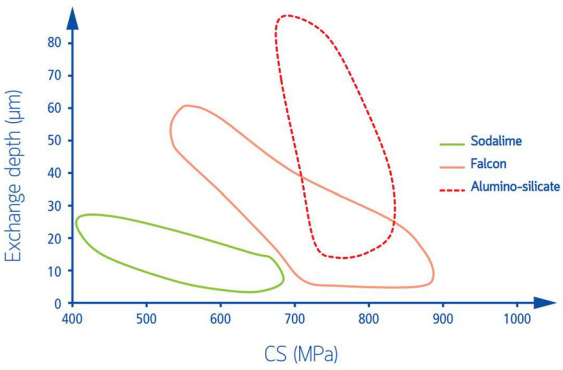

Fig. 2 Potential residual stress build-up

- Capability of monotonic load increase;
- Control of the loading rate;
- Capability of controlling the movement within a given degree of accuracy;
- Rollers fit for the purpose (i.e. that allow free rotation and avoid stress concentration).

The load from the equipment can be easily converted into stress by using Euler–Bernoulli linear elastic theory in the small deformation field. In this case the stress within the loading span is unidirectional and uniform. If thin glass were to be tested with the 4 PB method it would very likely deform beyond the small deformation field triggering non-linear behaviour (Maniatis et al. 2014). Practically, this will lead to the stresses being no longer unidirectional, with values varying across the width of the specimen: this is known as the 'Poisson's effect' (Fig. 3). Furthermore, in the extreme cases where the glass is very thin (i.e. < 1.1 mm) and very strong (i.e. chemically strengthened) the deformation will be so large that there will be the risk that the glass could slip out of the supporting rollers before it fractures.

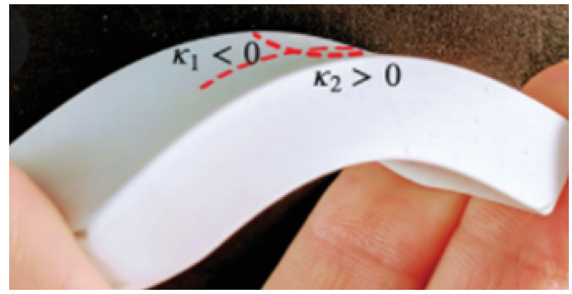

Fig. 3 Large deformation induced Poisson's effect

The standardized 4 PB method (EN 1288-3, 2016) proposes to use a correction factor when the Poisson's effect comes into play, but no solution can be found for the glass slipping out of the support. That is why researchers have worked to find alternative ways for testing thin glass. Neugebauer (2016) and Maniatis et al. (2014) suggested that bending with constant radius would be the most promising alternative for testing thin glass. Oliveira Santos et al. (2018) modelled and experimented various tests methods, including pure tensile test, but each type had a significant drawback. More recently, Galuppi et al. (2022) proposed a novel testing apparatus capable of twisting the glass, whilst Peters (2019) practically advanced in the development of a testing equipment to test glass for bending with constant radius, the clamp bender (CB). The simplicity and reliability deems the clamp bending the most promising method in terms of simplicity and reliability for thin glass testing. Clamp benders are not commercially available, but TU Darmstadt, TU Dresden and the R&D centre of AGC have autonomously and independently developed and in-house manufactured a clamp bender each, based on the same principles but with distinct differences between them. The three institutions joined their forces with the common goal of paving the way for a clamp bending method. The research method combined the theory related to bending with constant radius with the established 4 PB testing methodology. Unlocking thin glass testing is a precondition to endorse the use of thin glass in architecture. Statistically meaningful test data of annealed and chemically strengthened Falcon glass were produced while validating the method and the equipment.

2 Specimens

The specimens for this study are made of Falcon glass (AGC Glass Europe) with a thickness of 1.1 mm. The glass was produced by the float process and subsequently laser cut to a specimen size of 30 × 216 mm. The laser cutting consists of filamentation laser: the laser perforates the glass in one pass at 170 kHz of frequency. The pass between the holes is 4 μm which allows an easy manual separation of the specimens from the main flat glass sheet. Part of the glass specimens were chemically strengthened whereas others were kept in annealed condition, resulting in three individual test series:

- AN: Annealed glass;
- CS-8 h: Chemically strengthened glass at 460 °C for 8 h;
- CS-24 h: Chemically strengthened glass at 460 °C for 24 h.

Each research institute tested a set of the three series above. The chemical strengthening was performed in a single batch for all the specimens for each setting.

The surface residual stress and the case depth were measured on a total of 15 specimens for each of the chemically strengthened series by means of a differential surface refractometer, model FSM-7000H by Orihara. The measurement procedure consisted of 3 measurements per side (air/tin) for each measured pane. In Table 1 are shown the minimum, maximum and average value of the measured specimens for each of the two chemically strengthened series.

3 Test methods

3.1 General description of the clamp bender

A clamp bender is a testing equipment that imposes an increasing curvature to a specimen from the flat position (i.e. curvature = 0) until fracture. The curvature is theoretically uniform across the specimen's length at any time, in other words, the curved shape is an arc with a constant radius. The specimen, in our case thin flat glass, is clamped at two opposite edges and coordinated translation and rotation force the desired curved shape.

The stress, σ, is calculated according to Navier's formula, as follows:

$$\sigma = \frac{M h_g}{2I} \tag{1}$$

with M the bending moment, h_g the glass thickness and I the second moment of area.

The bending moment is function of the second moment of area, I, the Young's modulus, E, and the radius of curvature, R. In turn, trigonometry can be used to re-write the radius of curvature as function of the effective length, L_e, and the angle of curvature of the clamp, α. This results the bending moment being equal to:

$$M = \frac{EI}{R} = \frac{2EI\alpha}{L_e} \tag{2}$$

By effective length is meant the free length of the specimen which effectively undergoes curvature. Hence it is equal to the total specimen length minus the length embedded within the clamps.

The movement of the clamp bender is controlled by the rotational angle increase, which is related to the stress rate as follows:

$$\dot{\alpha} = \frac{\dot{\sigma} L_e}{E h_g} \tag{3}$$

The movement of the translation is related to the angle at any time and would vary according to the geometry of the clamp bender, notably the relative position between the axis of the shafts and the glass itself.

The specimens ought to be dimensioned considering that:

- The specimens must fracture before the motors arrive at the end of the stroke. This calls for small specimens, but the size must be considered depending on the expected glass resistance;
- The Poisson's effect is minimized with narrow specimens. However, if ground edge is to be tested, it ought be considered that the current industrial capability to grind 0.5 mm thick glass calls for a minimum width of 200 mm. Laser-cut edge can produce narrower specimen, instead.

Table 1 Results of the surface compressive pre-stress measurements

Surface compressive pre-stress (MPa)						DoL (μm)					
Air side			Tin side			Air side			Tin side		
Min	Max	Avg	Min	Max	Avg	Min	Max	Avg	Min	Max	Avg
519	568	558	504	525	513	46	47	46	43	44	43
411	476	445	402	422	412	74	78	76	69	80	78

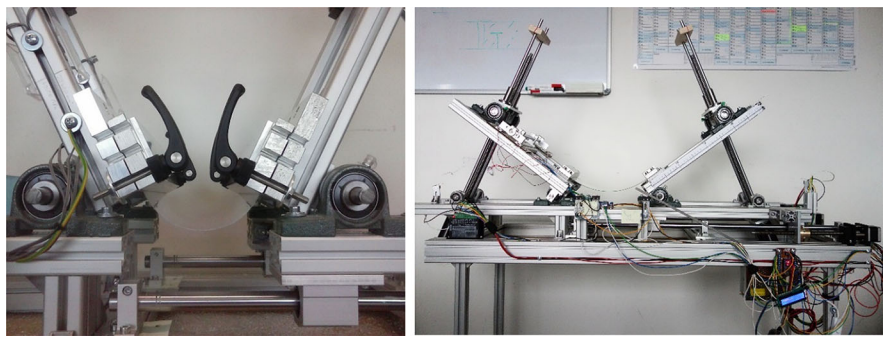

Fig. 4 Test setup at TU Darmstadt. Left: clamping area with a 0.5 mm specimen at over 300 MPa. Right: full machine view

3.2 Clamp bender developed at TU Darmstadt

The test setup of TU Darmstadt is depicted in Fig. 4.

The setup consists of two main aluminium extrusion profiles on which the two glass clamping units are mounted. One of the clamps including the lever arm is fixed in place and can only rotate around one bearing point, while on the other side of the machine, the clamp, the lever arm and the support structure for the rotation-inducing motor are mounted on a movable sled controlled by motors.

The lever arms for the rotational movement have a length of about 300 mm, and a ball screw with a stepper motor on the lower end is mounted between the end of the lever arm and the support structure using bearings to enable rotation of the glass clamps.

The movable sled is mounted on two linear steel shafts using linear bearings. Its horizontal movement is controlled by two spindles, one near each linear rail, driven by stepper motors.

The clamps are mounted on the lever arm with an offset of the glass clamping point of approximately 60 mm vertically and 30 mm horizontally from the bearing's rotational axis. In comparison with the two other testing setups, this allows the clamps to vary in width since they are not restricted by the rotational bearings. The clamps are milled from aluminium, and depending on the required width of the specimen, the thickness of the material varies between 10 and 30 mm to minimize deformation. The clamps are closed by one lever screw on each side, allowing for quick change of the specimens.

The stepper motors are NEMA 17 motors for the horizontal screws and NEMA 23 motors for the rotational screws, which (like the rest of the machine) are dimensioned to allow for a theoretical bending moment of over 1kNm. The motors are driven by 2-phase 12 V 4A stepper drivers controlled by a ATMEGA328P microcontroller (Arduino Nano). The microcontroller simultaneously also reads the data from the force sensors and input switches as well as buttons, controls the display and outputs data to a computer using serial connection. Timing all tasks on the single-thread processor proved challenging but possible.

To control each test, four input parameters are required: thickness of the specimen, span between the clamps (= testing length), Young's modulus and stress increase rate in MPa/s. Based on these inputs, all motor movement calculations are done by the software based on elastic beam theory and basic trigonometry.

The rotation, bending moment and calculated stress are output to the machine display and to the computer at a rate of 4 Hz resulting in one recording with every stress increase of 0.5 MPa. While higher data rates

would be possible, it was decided that this data rate was sufficient for glass with strengths of up to several hundred MPa.

To detect the fracture of the specimen, four strain gauges (Wheatstone bridge) are attached to one lever arm, measuring the deformation of the arm via a 24-bit A/D converter. The resulting bending moment is calculated by the microcontroller and output to the computer where, after the test is completed, the sudden change in bending moment is used to determine the fracture stress. The strain gauges have been tested to be sensitive enough to reliably detect fracture for specimen with thickness of 0.27 mm. Lower thicknesses might also be feasible.

3.3 Clamp bender developed at TU Dresden

A schematic representation of the test setup at TU Dresden is depicted in Fig. 5 and a photo is shown in Fig. 6.

The setup consists of two alloy shafts which are mounted via ball bearings on two alloy base plates. One of these base plates is fixed in position whereas the other can freely slide over an industrial rail system. The friction between the baseplate and the rail system is measured to be 500 N and is compensated for by a hanging weight on a pulley system that pulls the baseplate forward.

The alloy shafts (ø 50 mm) are provided with rounded slotted holes (40 × 10 × 10 mm) in which the thin glass specimens are mounted. To do so, the ends of the thin glass specimens are first provided with polymer caps. These polymer caps are made of a Polyethylenimine (PEI) blocks with slots of 40 × 8 × 1.2 mm in which the thin glass specimens are inserted. The dimensions of the polymer caps themselves are such that they tightly fit into the slotted holes in the alloy shafts (i.e. the thickness of the PEI caps is 0.1 mm smaller than the width of the slotted holes).

The shafts on the base plates can be rotated simultaneously by means of two stepper motors which are connected to the shafts directly via a gear drive with ratio 2:1 (i.e. one rotation of the stepper motor results in a half rotation of the shaft). The stepper motors (brand Sorotec type 110BYGH250C) have a maximum torque capacity of 22 Nm and their full rotation is divided into 200 steps. The stepper motors are operated by means of a Arduino Uno Rev. 3 Board and a stepperdriver model Leadshine EM705 digital which can steer the motor with up to 102,400 microsteps per rotation.

When the alloy shafts are rotated by the stepper motors, the thin glass specimen bends upwards. Due to this bending action the free sliding baseplate will move towards the fixed base plate. This movement is assisted by means of a hanging weight of 1.0 kg on the pulley system. Rotation of the shafts is continued until fracture of the thin glass specimens.

During the tests the horizontal movement of the free sliding base plate is measured by means of a linear displacement sensor. Also, the rotation of the shaft on the fixed base plate is measured by means of a turning sensor. All signals are acquired at a rate of 5 Hz, which results in an accuracy of recording of 0.1 degree (i.e. that is the smallest angle that can be measured). During the test, the event of glass fracture is evident and typically associated with collapse of the specimen. The fracture of the glass can be detected either by:

- a sudden acceleration of the sliding base plate. This case is more obvious for specimens breaking at a low rotation angle, i.e. annealed glass;
- a sudden increase of the rotation speed as measured by the turning sensor, due to sudden elastic force release upon glass fracture especially. This case is more obvious for specimens breaking at high rotation angles, i.e. chemically strengthened glass.

3.4 Clamp bender developed at AGC

The AGC equipment is characterized by two stepper motors: the right motor rotates only, whilst the left motor translates and rotates. A shaft with clamps is attached to each motor. The glass is held in the clamp so that the plane of rotation is parallel to the ground (Fig. 7). With this setup the deformation due to self-weight is negligible. The glass is positioned within the clamps with an offset in the x, and y direction, (x_1 and y_1 respectively) with respect of the axis of rotation of the shafts. Consequently, the translation of one motor must verify the following equation at any time:

$$d = L_e \frac{\sin\alpha}{\alpha} + 2\cos\alpha x_1 + 2\sin\alpha\left(y_1 + \frac{h_g}{2}\right) \qquad (4)$$

With d being the distance between the motor's axis.

The rotation of the two motors is synchronised. The shafts are shaped in order to maximise the rotational

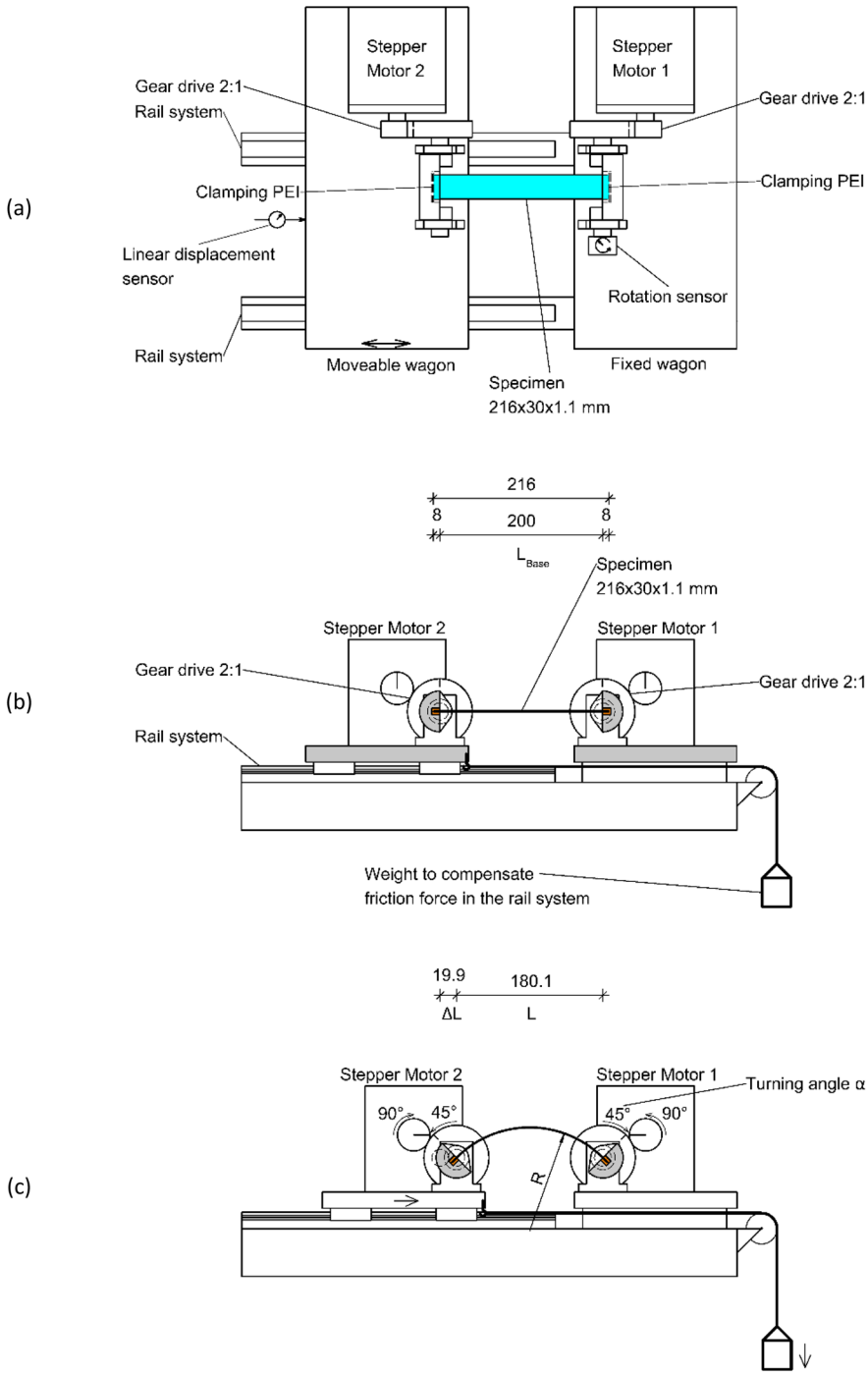

Fig. 5 Schematic representation of the test setup at TU Dresden; **a** top view; **b** side view, at starting position of 0° rotation angle; **c** side view, at 45° rotation angle

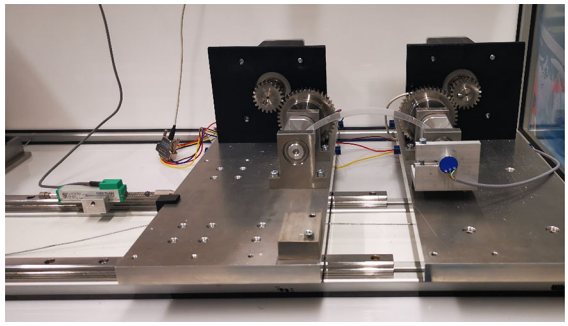

Fig. 6 Test setup at TU Dresden

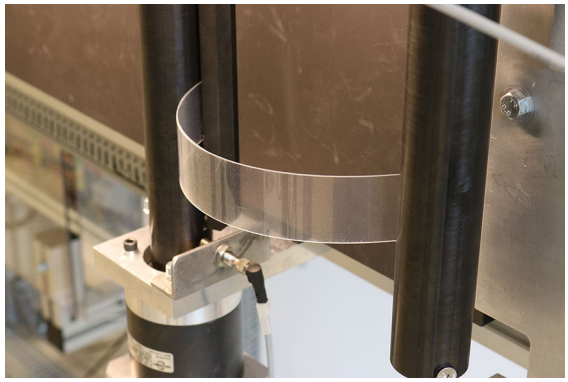

Fig. 7 AGC's clamp bender

angle. As a result, they can apply a rotational angle of 160° as long as the maximum torque that the motor can exert (i.e. 40 Nm) is not exceeded.

Rulers on the side of the clamps allow a precise positioning of the specimen with its long edge to be parallel to the translation. Furthermore, adequately positioned spacers allow even and sufficient clamping pressure on the specimens. The maximum clamping depth is 8 mm for each side, although the specimens can hang out of the clamps, providing that they would not collide with other parts of the equipment during the testing. This situation is normally avoided. The equipment can house specimens with maximum length of 1000 mm, maximum width of 200 mm and maximum thickness of 4 mm.

The fracture is detected by recording the video of the test with a multi camera capture software. The videos captured by the multi camera are the clamp bender with its specimen in testing and the screen of the software that controls the clamp bender, which includes the rotational angle. The video of the clamp bender in action is shot by the embedded camera of the pc in order to minimize latency. The field of capture is such to include the full specimen with the black background. A LED strip ensures uniform and adequate lighting conditions to easily detect the fracture. When the specimen breaks the test is manually stopped or else a safety stop is activated if the clamps reach the end of the stroke. The exact angle at fracture is read from the software display when the first frame with the fractured specimen appears. The angle at fracture is used to calculate the stress at fracture following Eqs. 1 and 2. In Fig. 8 are shown two consecutive frames, before and after fracture, of the layout of the multi camera capture software. The camera works at 30 fps, hence, the accuracy will depend on the speed of test. In the case of 2 MPa/s, this leads to an accuracy of 0.06 MPa.

3.5 Test procedure and settings

The clamp bending tests started by positioning the glass in the clamps. From each side, 8 mm of the total length were fastened in the clamps leaving the effective tested length equal to 200 mm. Care was taken in order to avoid that the clamp would provoke stress concentration or uneven pressure application. The test was performed at a loading rate of 2 MPa/s, which for the tested specimen's geometry equals to approximately 0.3°/sec. The specimens were positioned so to have the tin face subjected to tension. A transparent adhesive film was applied on the air side of the glass with the purpose of holding the fragments together after fracture and hence to identify the origin of fracture. The angle at fracture was determined, from which the fracture stress was calculated according to Eqs. 1 and 2.

3.6 Poisson's effect

The uniformity of stress along the specimen during the clamp bending test is only apparent: the large deformation induce bending along the width of the specimen that is function of the aspect ratio and the amount of curvature, just as per the 4 PB method. A finite element (FE) analysis was performed in order to assess the impact of this non-linearity and determine the discrepancy between the calculated stresses and the actual stress. It consisted of a symmetric nonlinear 3D FE model representing one quarter of a tested 1.1 mm thick

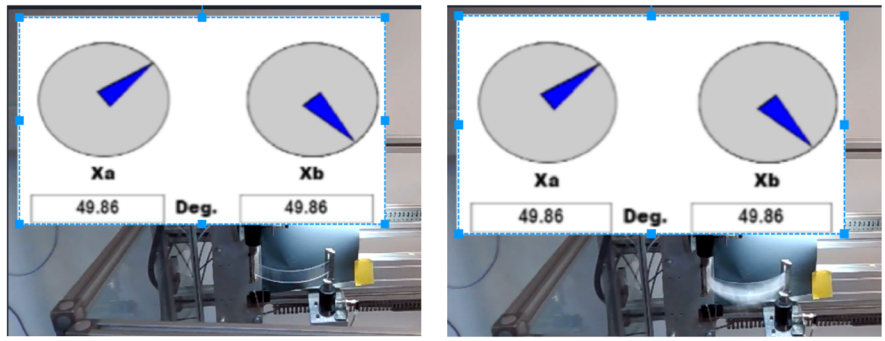

Fig. 8 screenshot of the multi camera software to detect fracture: left) frame before fracture; right) frame at fracture: they are both reading 49.86 as angle of curvature

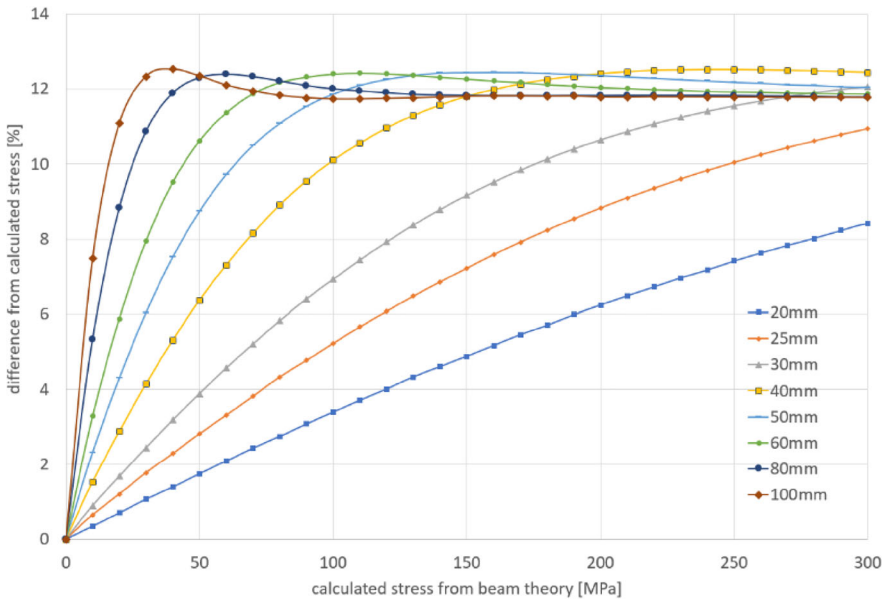

Fig. 9 Discrepancy between calculated and actual edge stress in the center of a 1.1 mm specimen with varying width (range 20–100 mm) due to the Poisson's effect, as calculated by FE

and 200 mm long glass specimen with a slowly increasing rotation applied to the segment inside the clamps. The result (Fig. 9) showed that the actual stress on the edges is higher than that in the center of the specimens. Furthermore, this difference is not constant along the length of the specimen and for the tested geometry is never above 12.6% in the worst case scenario. In this study it was chosen to take the test data as they are, considering that the results are on the conservative side, but a detailed study to understand how to address the discrepancies due to the Poisson's effect ought to be considered.

4 Results

Weibull plots are shown in Figs. 10, 11, 12 and 13. The Δx-y interval of Figs. 10, 11 and 12 is the same, so that the slope of the best-fit Weibull plot is comparable amongst them. The test results are shown in Table 2, grouped by research institute as well as all data aggregated. Typical images of the fractured specimens are shown in Fig. 14.

5 Discussion

The development of the clamp bender as well as the testing procedure was done by considering the EN 1288–3 as a reference. As such all the three test setups fulfil the following specifications:

- Increasing the stresses monotonically from zero to fracture;
- Controlling the speed of stress increase;
- Controlling the movement with a given degree of accuracy;

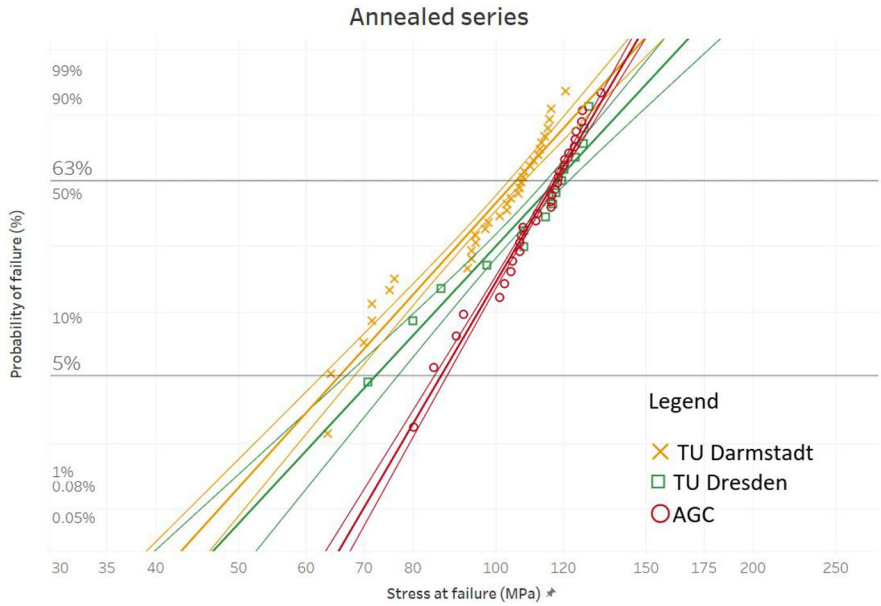

Fig. 10 Weibull plots of the annealed series: by testing institute

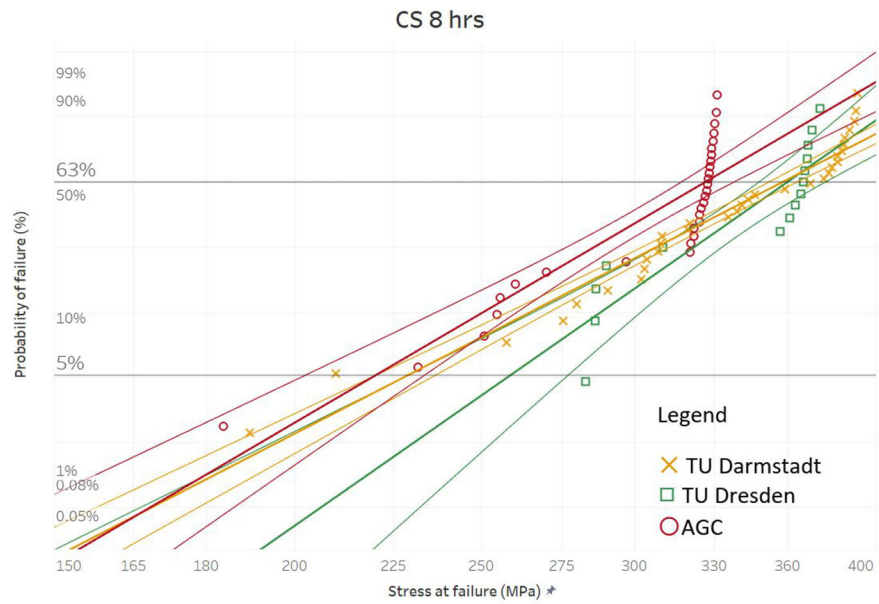

Fig. 11 Weibull plots of the chemically strengthened series for 8 h at 460 °C: by testing institute

- Imposing boundary conditions that match the theory.

Furthermore, the following points were also addressed according to the EN 1288–3:

- Speed of test set to 2 MPa/s, to limit the slow crack growth;
- Tested length set to 200 mm;
- Apply an adhesive film to hold the fragments together after fracture.

These elements can be the basis for a standardization of the clamp bending test. Nevertheless, care should be taken with regard of the tested length. The value of 200 mm was here chosen to enable a direct comparison between the clamp bender test results with results of

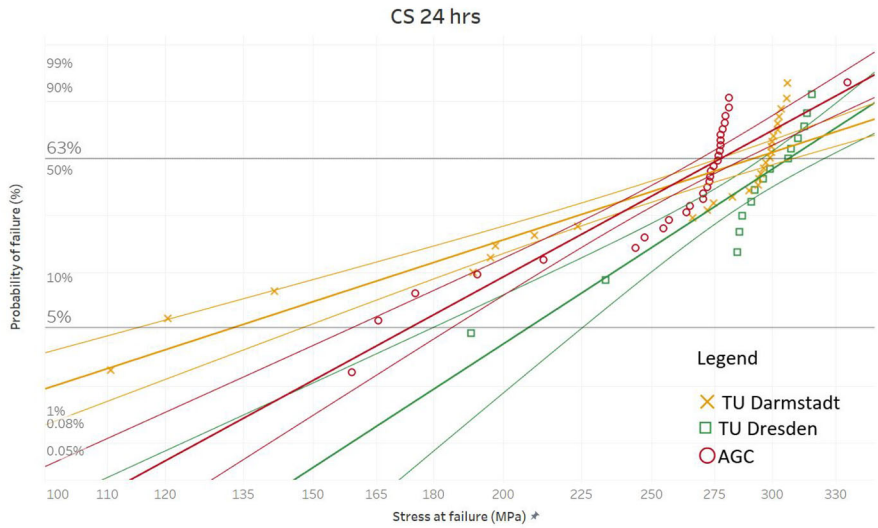

Fig. 12 Weibull plots of the chemically strengthened series for 24 h at 460 °C: by testing institute

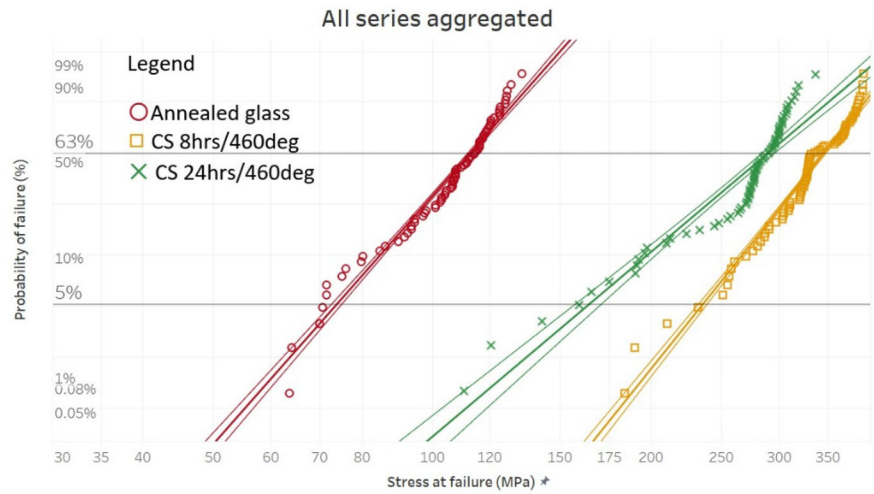

Fig. 13 Weibull plots of all the series, all data together

the standardized 4 PB method wherein the span under constant stress (i.e. the distance between the loading rollers) is also 200 mm. However, the width of the specimens for the standardized 4 PB test is 360 mm, in contrast to the 30 mm of the specimen width used in this study. Therefore, the comparison still holds if only the edge flaw population is considered. The rigor of this assumption deserves to be evaluated further.

The Poisson's effect is a phenomenon that ought to be taken into account when striving for accuracy. From a practical point of view, simplified methods ought to be considered in order to account for the Poisson's effect. The simplification might consist of standardizing the specimen size along with proposing a graph providing a correction factor. The correction factor approach is already taken into account by the EN 1288-3 when large deformation occurs. Nevertheless, not accounting for the Poisson's effect is on the conservative side, therefore, when dealing with a new product such as thin glass, such extra safety margin surely may be considered beneficial.

Testing the same glass with three different test setups gives the opportunity to gain confidence on the testing equipment as well as on the test data. When considering the Weibull parameter θ, it can be observed that the values are very similar one another (see Table 2),

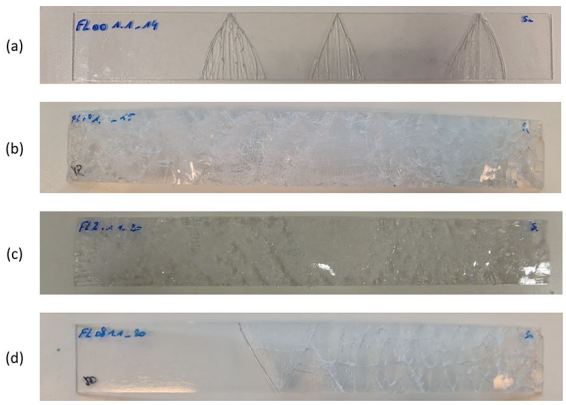

Fig. 14 Fractography on fractured specimens: **a** annealed glass; **b** chemically strengthened 8 h; **c** chemically strengthened 24 h; **d** unusual fracture pattern of a chemically strengthened for 8 h

despite that the number of tested specimens was different for each testing institute. For example, the annealed specimens show a bending strength of 116 MPa for the series tested at TU Dresden and AGC, which is about 11% higher than the value of 104 MPa for the series tested at TU Darmstadt. Considering the series chemically strengthened for 8 h, the difference between the combined data of all series and the data for the individual series per equipment does not differ by more than 19 MPa, (see Table 2), which corresponds to a variation even lower than the annealed series: about 7%. When considering the characteristic bending strength, $f_{g;k}$, the difference increases significantly for the 24 h strengthening series, with for example TU Darmstadt obtaining 147 MPa and TU Dresden 216 MPa. The difference is slightly less relevant for the annealed series, with AGC finding 82 MPa in contrast to the 63 and 67 MPa found by TU Darmstadt and TU Dresden, respectively. However, the characteristic values of the 8 h strengthening series are fairly close one another, with the largest discrepancy being only 19 MPa between the all data and the TU Dresden series. The reason for discrepancy should not be searched only in the equipment itself. In practice the glass was:

- Shipped further from AGC to Dresden and Darmstadt, respectively, so it might have suffered a further damage due to handling and transport;
- The chemical strengthening: the larger data scattering in the 24 h series suggests a more varied flaw population, that might arise during the longer chemical strengthening process.

The resulting Weibull plots should also be looked at with care. In particular, the plots relative to the chemically strengthened glass classified by testing institute (Figs. 10, 11 and 12) show clearly that for each series the many data points fall outside of the confidence interval of the best-fit curve. This discrepancy is commonly interpreted as if there are two flaw populations that would lead to two distinct slopes. No clear explanation was found for this phenomenon, but given that this discrepancy is mainly observed with the chemically strengthened series, it may be related with the specific chemical strengthening procedure applied for the specimens in this study and should be investigated further.

All in all, the data suggests that the clamp bender provide reliable and repetitive data. With this being the first study with actually tested specimens, further fine-tuning is needed to improve the procedure and the results.

The first sets of thin glass chemically strengthened with laser-cut edges were tested. This showed a characteristic bending stress of 229 MPa for the 8 h series. Lower values were observed for the 24 h series, with the lowest obtained by TU Darmstadt at 147 MPa. The annealed series performed well above the commonly expected 45 MPa.

Further work is needed to consolidate the procedure, more specifically:

- Standardize the specimen size so to have a statistical distribution of the surface flaws comparable with other standardized tests (i.e. the 4 PB method);
- Define how to account for the Poisson's effect by a combination of FE simulations as well as testing with strain-gauges.

6 Conclusion

Three clamp benders were autonomously and independently developed by TU Darmstadt, TU Dresden and AGC. The equipment was built in order to comply with established testing setup and procedure such as the 4 point bending method. Three series of thin glass, two of which were chemically strengthened for 8 h and 24 h, respectively, at 460 °C, were tested by each equipment. The good matching of the results coming from different equipment put the basis for a simple and reliable method for testing thin glass. Furthermore, it was shown that 1.1 mm thin glass with laser cut

Table 2 Test results

Series	Testing institute		As-tested		
		# of specimens	θ (MPa)	β	$f_{g;k}$ (MPa)
AN	TU Darmstadt	32	104	8.0	63
	TU Dresden	15	116	8.6	67
	AGC	30	116	11.3	82
	All data combined	77	112	8.3	73
CS-8 h	TU Darmstadt	32	355	8.5	222
	TU Dresden	15	357	13.4	248
	AGC	30	320	14.0	237
	All data combined	77	343	8.8	229
CS-24 h	TU Darmstadt	32	282	6.5	147
	TU Dresden	15	301	14.4	216
	AGC	30	273	8.8	173
	All data combined	77	283	8.0	180

edges and chemically strengthened for 8 h can have a characteristic bending strength equal to 230 MPa. Also annealed glass performed outstandingly, almost doubling the expected performances of regular annealed glass. A broader glass community discussion on the subject is needed to move towards a standardization of the clamp bending as the prevailing method for testing thin glass. The results presented in this paper provide a solid basis for further discussions and developments.

Acknowledgements The authors acknowledge Arthur Comblen, Jean-Philippe Biard, Jean-Marco Noiret for conceiving, designing and building the AGC's clamp bender.

Declarations

Conflict of interest On behalf of all authors, the corresponding author states that there is no conflict of interest.

References

ASTM E1300. Standard practice for determining load resistance of glass in buildings (2012)

Bartholomew, R.F., Garfinkel H.M.: Chemical strengthening of glass. In: Uhlmann, D.R., Kreidl, N.J. (eds.) Glass Science and Technology, Vol. 5. New York (1980)

Burggraaf, A.J., Cornelissen, J.: The strengthening of glass by ion-exchange. Part I stress formation by ion diffusion in alkali aluminosilkicate glass. Phys. Chem. Glasses **5**, 123–129 (1964)

Cervio, M., Muciaccia, G., Rosati, G.: Impact performance of thin glass-polycarbonate composite panels. In: challenging glass conference proceedings, vol 5 Ghent: Belis, Bos & Louter, (2016)

Pfarr, D., et al.: Dünnglas-Verbundelemente mit additiv gefertigtem polymerkern: formfindung, fügeverfahren und untersuchung der Biegesteifigkeit. Wiley Online Library, **90**, 507–516

Datsiou, K.C., Overend, M.: Artificial ageing of glass with sand abrasion. Construct. Build. Mater. **142**, 536–551 (2017)

EN 1288-3 Glass in building-determination of the benging strength of glass—part 3: test with specimen supported at two points (four point bending) (2016)

Galuppi, L., Riva, E.: Experimental and numerical characterization of twisting response of thin glass. Glass Struct. Eng. **7**(1), 45–69 (2022)

Hanig, J., Bernhard, W.: Experimental investigations and numerical simulations of innovative lightweight glass-plastic-composite panels made of thin glass and PMMA. Glass Struct. Eng. **6**, 249–271 (2021)

Maniatis, I., Nehring G., Siebert G.: Studies on the strength of thin glass. In: IABSE symposium Report. Madrid, (2014)

Lambert, H., O'Callaghan, J.: Ultra-thin high strength glass research and potential applications. Glass Perform. Days. 95–99 (2013)

Louter, C.P., et al.: Adaptive and composite thin glass concepts for architectural applications. Heron **63**(1), 199–218 (2018)

Maniatis, I., Nehring, G., Siebert, G.: Studies on determining the bending strength of thin glass. Struct. Build. **169**, 393–402 (2014)

Overend, M., et al.: Glass reinforced glass. Glass Perform. Days. (2013)

Neugebauer, J.: Determining of bending tensile strength of thin glass. Challeng. Glass Conf. **5**, 419–428 (2016)

Neugebauer J., et al.: Movable thin glass elements in facades. In: Challenging glass, vol 6, Delft, Belis, Bos & Louter (2018)

Oliveira Santos, F., Louter, C., Ramoa Correia, J.: Exploring thin glass strength test methodologies. Challeng. Glass Conf. Proc. **6**, 713–724 (2018)

Schossler, N.: Thin glass as cold bent laminated panels in architectural applications. MSc Thesis, TU Delft, (2018)
Silveira, R.R., Louter, C., Klein, T.: Flexible transparency-a study on adaptive thin glass facade panels. Challenging Glass, vol. 6. Delft, Belis, Bos & Louter, (2018)
Pennetier, S., Ronfini, A., Stoddard J.: Advances in prototyping with ultra-thin glass. Glass Performance Days. Tampere (2019)
Peters, T., Jaschke, S., Schneider, J.: Thin glass in membrane-like structures-applications, modelling and testing. In: IASS annual symposium-form and force. Barcelona, International Association for Shell and Spatial Stractures, (2019)
Weimar, T., López, S. A.: Research on thin glass-polycarbonate composite panels. In: challenging glass. Vol. 6, TU Delft Open, (2018)
Zaccaria, M., Gillon, X.: scaling thin glass use to the architectural world. In: Glass performance days. Tampere, pp. 320–323, (2019)
Zaccaria, M., Overend, M.: Thermal healing of realistic flaws in glass. J. Mater. Civ. Eng. **28**(2), (2016)
Zaccaria, M., et al.: Chemically strengthened glass for architectural applications. In: engineered transparency. Wiley, Dusseldorf, (2021)